

Microtubule-associated protein 4 (MAP4) regulates assembly, protomer-polymer partitioning and synthesis of tubulin in cultured cells

H. Lan Nguyen¹, D. Gruber² and J. Chloë Bulinski^{1,2,*}

Departments of ¹Pathology and ²Anatomy and Cell Biology, Columbia University, College of Physicians and Surgeons, BB1213-630 W. 168th St, New York, NY 10032-3702, USA

*Author for correspondence (e-mail: jcb4@columbia.edu)

Accepted 3 April; published on WWW 26 May 1999

SUMMARY

We depleted MAP4, a ubiquitously expressed microtubule (MT)-associated protein previously shown to be capable of stabilizing MTs, from HeLa cells by stably expressing antisense RNA. These HeLa-AS cells, in which the MAP4 level was decreased to 33% of the wild-type level, displayed decreased content of total tubulin (65% of the wild-type level). The partitioning of cellular tubulin into protomer and polymer was altered in HeLa-AS cells: polymeric tubulin was decreased to 46% of the level in control cells, while protomeric tubulin was increased to 226% of the level in control cells. Tubulin protein synthesis was decreased, consistent with the tubulin autoregulation model, which

proposes that tubulin protomer inhibits its own synthesis. Following release from drug-induced depolymerization, MTs in HeLa-AS cells reformed more slowly, and showed an increased focus on the centrosome, as compared to control cells. HeLa-AS cells also appeared to be less bipolar in shape and flatter than control cells. Our data suggest that MAP4 regulates assembly level of MTs and, perhaps through this mechanism, is involved in controlling spreading and shape of cells.

Key words: MT nucleation, Tubulin monomer, Cell morphology, MTOC, Microtubule polymerization, Autoregulation

INTRODUCTION

In cells, the tubulin pool is partitioned into unpolymerized tubulin (tubulin protomer) and assembled tubulin, or microtubules (MTs), in which tubulin subunits are polymerized into long fibers that are further organized into a cytoplasmic MT network. Both the intracellular level of MTs and the proper partitioning of tubulin into protomer and polymer pools are thought to be important for physiological functions.

The behavior of MTs both in vitro and in vivo is best described by the dynamic instability model (Mitchison and Kirschner, 1984), which is based on the observation that individual MTs undergo stochastic alternations between periods of polymerization and depolymerization. In contrast to the original model of Oosawa and Asakura (1975), which modeled MT behavior by analogy to that of other linear polymers, the dynamic instability model proposes that MTs exist in a dynamic, rather than a true, equilibrium with tubulin protomers (Mitchison and Kirschner, 1984). Consequently, partitioning between protomeric and polymeric tubulin would be expected to vary as a function of number of nucleating sites, rate of MT regrowth, and frequency of transition between growing and shrinking phases (Mitchison and Kirschner, 1984). Thus, the dynamic behavior of MTs is predicted to impact upon the steady-state level of assembled MTs.

One mechanism by which cells are believed to modulate MT dynamics and assembly is through proteins associated with the

MT lattice. A subset of microtubule-associated proteins (MAPs) has been classified as assembly-promoting, since each binds to MTs and stimulates their polymerization in vitro (Mandelkow and Mandelkow, 1995). The assembly-promoting MAPs include tau and MAP2, expressed abundantly only in nervous tissue, and MAP4, expressed ubiquitously in non-neuronal cells (Bulinski and Borisy, 1980b; Parysek et al., 1984; Huber and Matus, 1990; Faruki and Karsenti, 1994; Bulinski, 1994).

MAP4 is a heat-stable protein of approx. 210 kDa that is the most abundant non-tubulin component of MTs in non-neuronal cells. MAP4 homologs have been identified in all vertebrates and in organisms as primitive as the nematode, *Caenorhabditis elegans* (Goedert et al., 1996; McDermott et al., 1996). MAP4 is a component of MTs performing many disparate functions, such as those that organize and transport organelles and vesicles in interphase cells, those that make up the spindle fibers during mitosis, and those that are involved in changing cell shape during differentiation (Bulinski and Borisy, 1980b; Parysek et al., 1984).

Biochemical studies have demonstrated the in vitro capacity of MAP4 to stabilize MTs and to dampen dynamic instability (e.g. Bulinski and Borisy, 1980a; Aizawa et al., 1991; Itoh and Hotani, 1994). Results of studies in which the cellular content of MAP4 was increased by transfection (e.g. Olsen et al., 1995; Nguyen et al., 1997) or microinjection (Yoshida et al., 1996), provide further support for the hypothesis that either full-length MAP4 or its MT-binding domain (MTB) can stabilize MTs in vivo. These findings

are notable, since recent evidence indicates that ability to increase MT stability by enhancing MAP4 expression may be physiologically significant. Sato et al. (1997) showed that heightened expression of MAP4 mRNA and protein preceded increases in number and stability of MTs in myocardium undergoing hypertrophy in response to pressure overload.

Although experiments in which MAP4 content was elevated demonstrated that MAP4 is capable of promoting MT stability (Olsen et al., 1995; Yoshida et al., 1996; Nguyen et al., 1997), we wished to assess the actual contribution of MAP4 to MT polymerization or dynamics in a cellular milieu containing other MAPs. To do so, it was necessary to examine the sequelae of reducing or ablating MAP4 in vivo. Insight into functions of both tau (Caceres and Kosik, 1990; Esmali-Asad et al., 1994) and MAP2 (Dinsmore and Solomon, 1991) have been acquired by antisense depletion. The defective neurite polarity in tau-deficient neuronal cells and the abnormal neurogenesis in MAP2-deficient cells demonstrated the importance of these MAPs in morphological changes. Interpretations of these results, however, were confounded by findings from another experimental system: mice in which tau had been genetically knocked out possessed no significant phenotypic abnormalities in neuronal development, axonal morphology or MT-dependent functions (Harada et al., 1994). These results highlight the challenge of using depletion to analyze protein function in the complex system of a whole animal, since the possibility of compensatory actions by other proteins precludes definitive assignment of functions to the protein that was ablated.

Previous studies by Mangan and Olmsted (1996) reported that expression of MAP4 antisense sequences in C₂C₁₂ muscle cells reduced the level of a minor, muscle-specific isoform of MAP4 protein and compromised myogenic differentiation. This result suggested that this specialized isoform of MAP4 functions in myogenic morphogenesis. In contrast, no previous studies using antisense or mouse knockout techniques have been applied to discern functions of the major, ubiquitously expressed form of MAP4. A strategy Wang et al. (1996) used to deplete MAP4 function was to microinject human fibroblasts with antibodies that inhibited MAP4's MT-binding. Unexpectedly, no abnormalities were observed in cell morphology, position of mitochondria, formation of mitotic spindles or turnover of MTs, suggesting that molecules functionally redundant with MAP4 might be present in fibroblasts, or that MAP4 actually does not play significant roles in the functions tested.

In order to ascertain the functions of MAP4 in living cells amenable to biochemical assays of MAP function, we used antisense expression to deplete MAP4 from HeLa cells. We show here that this approach allowed us to generate and characterize populations of cells deficient in the major, ubiquitously expressed form of MAP4. These cells exhibited obvious abnormalities in their MT system and in their morphological characteristics.

MATERIALS AND METHODS

Materials

Unless noted, chemicals, plasticware and supplies were obtained from Sigma (St Louis, MO) or Fisher Scientific (Tustin, CA). Tissue culture reagents were purchased from Gibco (Gaithersburg, MD), immunochemicals from Organon Teknica (West Chester, PA),

restriction enzymes and Taq Polymerase from Promega Biotech (Madison, WI) and radioisotopes from DuPont NEN Research Products (Boston, MA).

Vectors and sequences

The MAP4 antisense construct was made by PCR, with full-length MAP4 cDNA as template. 5' and 3' primers, 5' AGTTGCTCG-AGTGCAGAATGGCTGAC and 5' TCTTCGCTAGCTTCAGTT-GGAGACCC, respectively, matched the MAP4 cDNA sequence nt59–392, with an *Xho*I site introduced at nt64 and an *Nhe*I site at nt387. PCR product was cloned into *Xho*I and *Nhe*I sites of pCEP4 (Invitrogen Corp., Carlsbad, CA). The MAP4 sense construct was prepared identically, except with *Nhe*I and *Xho*I sites in the 5' and 3' primers, respectively. PCR reactions used a Perkin Elmer-Cetus Thermal Cycler, as follows: 30 seconds at 95°C, 1 minute at 45°C, 1 minute at 72°C for five cycles, followed by 30 cycles with the same conditions, except using 1 minute at 55°C for the annealing step.

The pGFP-MTB chimera was made by PCR, with 5' and 3' primers, 5' GGAGAGGGTACCCGGGACTTCATTGCC and 5' GGGACCC-GGGAGACGACACCAGA, respectively, and pGEM7MAP4 (form IV) as template (Chapin et al., 1995). Primers corresponded to the MAP4-MTB sequence nt52–1714, with introduced 5' and 3' *Kpn*I and *Sma*I sites. The PCR fragment was cloned in-frame with green fluorescent protein (GFP) coding sequence, in pEGFP-C1 (Clontech, Palo Alto, CA).

Culture and transfection of HeLa cells

Six-well dishes of HeLa-WT cells, in DMEM with 10% calf serum (Hyclone Laboratories, Inc., Logan, UT) were plated at a density of 8×10^5 cells per well, about 24 hours before transfection, and were rinsed once with serum-free, antibiotic-free DMEM. Sterilized DNA (2 µg) was combined with Lipofectamine (10 µl; Gibco, Gaithersburg, MD), in 200 µl DMEM, pre-incubated for 45 minutes at room temperature, mixed with 800 µl of DMEM, and applied to each well. After 24 hours, medium was replaced with DMEM with serum; hygromycin B (150 µg/ml) was added 48 hours later. Stable transfectants were selected by growing cells in 150 µg/ml hygromycin B for 3 weeks; 40 colonies of each were isolated. HeLa-AS and HeLa-S cells were cultured in the presence of hygromycin B (100 µg/ml) to prevent plasmid loss. Retransfection of HeLa-AS cells with pEGFP-N1 encoding GFP-MTB chimera was performed identically to the above, except that selection of transfectants was performed in the presence of geneticin (G418), and cells were sorted by FACS 1–2 weeks after transfection.

Northern blotting

Total RNA, isolated with Ultraspec Reagent (Biotecx Labs, Inc., Houston, TX), electrophoresed according to Kroczek and Siebert (1990), except with 1.1% formaldehyde in the running buffer, was blotted, and replicas (Sambrook et al., 1989) were fixed in a Spectrolinker XL-1000 UV-Crosslinker (Spectronics Corp., Westbury, NY). Blot membranes were prehybridized at 65°C for 15 minutes in 6 ml Rapid-hyb buffer (Amersham Life Sciences, Arlington Heights, IL), hybridized at 65°C for 2 hours in a Micro Hybridization Incubator (Robbins Scientific, Sunnyvale, CA), and then probed with antisense MAP4 riboprobe. Probe was made from *Xba*I-linearized pBluescript-Hep1 cDNA (Chapin et al., 1995) containing the 3'–1.1 kb of MAP4 cDNA, with ³²P-UTP and T7 RNA polymerase, using an Ambion MAXIscript kit (Ambion, Inc., Austin, TX), and removing unincorporated nucleotide with Sephadex G-50. Membranes were washed at 70°C for 15 minutes; once with 5×SSPE (Sambrook et al., 1989), 0.5% SDS; twice with 1×SSPE, 0.5% SDS; and twice with 0.1×SSPE, 1% SDS, and exposed with an intensifying screen (2 hours, –80°C).

To detect GAPDH transcript, a [γ -³²P]dCTP-labeled, double-stranded cDNA probe was synthesized by random priming (Decaprime Kit; Ambion Inc., Austin, TX) of GAPDH cDNA (gift from Dr Ricardo Dalla-Favera, Columbia University, NY). GAPDH

blots were handled as above, except they were washed only once with 0.1×SSPE, 1% SDS (65°C, 15 minutes) and were exposed for 3 days at -80°C, with no intensifying screen.

RT-PCR of MAP4 sense and antisense transcripts

To detect antisense transcripts, 2 µg total RNA was added to 0.5 µl 100 mM methyl mercury hydroxide, the volume was adjusted to 5 µl with RNase-free water, and the mixture was placed at 24°C for 10 minutes to denature RNA. 2.5 µl 140 mM β-mercaptoethanol were added and the mixture was incubated (5 minutes, 0°C) to inactivate the methyl mercury hydroxide. 15 U RNasin, 3 µl 5×MMLV reverse-transcriptase (MMLV-RT) buffer, 2 µl 100 mM DTT (all from Promega, Madison, WI), and 1 µl 0.5 mg/ml random hexamers (Boehringer-Mannheim, Indianapolis, IN) were added, and the volume was brought to 15 µl. After primer annealing (5 minutes, 24°C), 2 µl 40 mM dNTP mixture (Boehringer-Mannheim, Indianapolis, IN), 1 µl MMLV-RT buffer, 1.5 µl water and 0.5 µl MMLV-RT enzyme were added, and reverse transcription proceeded (90 minutes, 37°C). To detect sense transcripts, the reverse transcription step was modified: 2 µg total RNA was mixed with 1.5 µl 1 mg/ml random hexamers (Boehringer Mannheim, Indianapolis, IN) in a volume of 11.5 µl, incubated (70°C, 15 minutes) and placed on ice. 4 µl 5×RT-buffer, 1 µl 100 mM dNTPs, 0.5 µl RNasin (40 units/µl), and 1 µl MMLV-RT (200 U/ml) were added and incubated for 1 hour at 37°C, and then for 3 minutes at 93°C.

PCR was performed on all samples, using the above conditions for 30 cycles, all with an annealing temperature of 55°C. To generate positive control products, pCEP4-MAP4-S and pCEP4-MAP4-AS were cut with *Xho*I, and 100 ng of each was used as PCR template. 5'-primer, with sequence 5' ATCTCTAGAAGCTGGGTACCA, was used to prime sequences downstream of the transcriptional start site of pCEP4 vector, (nt522, common to both sense and antisense transcripts). 3'-primers utilized were 5' AGAATGGC-TGACCTCAGTCTT, beginning at nt73 of MAP4 cDNA, for antisense transcript, and 5' TGGAGACCCTGTAGTATCGCT, starting at nt375, for sense transcript. MAP4 sense or antisense transcript yielded RT-PCR products of predicted sizes of 335 and 338 bp, respectively.

Immunoassays of MAP4, tubulin and vimentin

Western blots, as described previously, used MAP4 antibody or anti-MTB antibody (Nguyen et al., 1997), β-tubulin antibody (a generous gift from Dr James Lessard, University of Cincinnati), or vimentin antibody (VIM-13.2, Sigma, St Louis, MO). MAP4 and tubulin were quantified as before (Nguyen et al., 1997). Immunofluorescence differed from Chapin and Bulinski (1991a) in that cells were cultured on fibronectin-coated coverslips (5 µg/ml; Boehringer Mannheim Corp., Indianapolis, IN). Microscopy and imaging were performed as described (Nguyen et al., 1997), except with 1 second exposures.

Quantification of MT polymer

The procedures of Gundersen et al. (1987) were modified slightly. Cells in confluent monolayers in 60 mm dishes were washed twice in Earle's buffered salt solution (EBSS) at 37°C, collected in 6 ml EBSS with a scraper, disaggregated and the suspension divided in half. After centrifugation (1000 rpm, 3 minutes), cell pellets were gently loosened and resuspended, using 3 ml MT-stabilizing buffer (MSB; 85 mM Pipes, pH 6.93, 1 mM EGTA, 1 mM MgCl₂, 2 M glycerol) for one tube and MSB containing 0.5% Triton X-100 for the other. After incubating (37°C, 2 minutes) and centrifuging at room temperature (2500 rpm, 3 minutes), an identical volume of SDS-gel sample buffer was added to pellets containing total cell protein (i.e. extracted in MSB alone) and MT polymer (i.e. extracted in MSB with Triton). Samples were boiled (15 minutes), centrifuged (room temperature, 14,000 rpm, 10 minutes) and snap-frozen. Protein assays of total cell protein samples ensured that 5 µg of each unextracted sample and an equal volume of the Triton-extracted companion sample were electrophoresed and immunoblotted.

Tubulin levels were quantified from blots of 1-20 µg extract protein (Chapin and Bulinski, 1991b); the percentage of tubulin in the polymer was defined as the ratio (tubulin in MT polymer sample) : (tubulin in total protein extract). To verify the extraction conditions, the percentage of polymer was determined in HeLa cells pre-treated for 2 hours with nocodazole (4 hours, 10 µM; no detectable polymer) or Taxol (4 hours, 2 µM; no detectable protomer) (Gundersen et al., 1987).

Assay of tubulin synthesis

Cells plated at identical densities in 6-well culture plates were washed once in warm medium (lacking methionine and glutamine; Mediatech, Herndon, VA) and each well was incubated in 2 ml medium for 20 minutes, then in 200 µCi ³⁵S-methionine (³⁵S-Met) in 250 µl medium, for 30 minutes. Medium was aspirated and 150 µl cold lysis buffer (25 mM Tris-Cl, pH 7.5, 0.4 M NaCl, 0.1% deoxycholate, 1% NP-40, 0.5% SDS and protease inhibitors) was added. Preparation of extract and determination of ³⁵S-Met incorporation from trichloroacetic acid (TCA)-precipitable radioactivity were performed as described (Cleveland et al., 1981). Tubulin was immunoprecipitated as follows: the extract from each well was precleared by preincubating with 20 µl normal goat serum for 1 hour on ice, adding 20 µl crude protein A, gently agitating (4°C, 1 hour), and centrifuging (2 minutes, 6000 rpm). Approximately 15-50 µl (10⁶ cpm) supernatant was immunoprecipitated with 5 µl anti-tubulin (X²; Gundersen et al., 1987) or with pre-immune serum, in 1 ml dilution buffer (50 mM Tris-Cl, pH 7.5, 150 mM NaCl, 0.1% NP-40, 1 mM EDTA, pH 8.0, 0.25% gelatin, 0.02% sodium azide). Samples were agitated (4°C, 1 hour), and 20 µl protein A-agarose beads, prewashed in dilution buffer, were added. After a 1 hour agitation at 4°C, samples were centrifuged. Pellets were washed twice (15 minutes, 4°C) in dilution buffer, then in Tris-buffered saline (TBS) with 0.05% NP-40 (thrice) and in TBS (once). Samples were electrophoresed, autoradiographed and quantified, as above.

Quantification of cell spreading

HeLa-AS and HeLa-S cultures in half-confluent 60 mm culture plates were washed four times with warm DMEM before viewing with a Nikon Eclipse-TE300 microscope, with a 100×/1.30NA Plan-Fluor objective. At least six phase-contrast images of fields of cells of each line, from two separate passages, were captured with a Micromax cooled-CCD camera (Princeton Instruments, Trenton, NJ) with a Kodak KAF1400 chip (Kodak, Rochester, NY). Images were processed with Metamorph software (Universal Imaging, West Chester, PA); dimensions were calibrated, the perimeter of each was traced, and the surface areas were graphed with SigmaPlot software (Jandel Scientific, San Rafael, CA).

Fluorescence-activated cell sorting (FACS)

To determine cell volume, cells were cultured until confluent, trituated, fixed and stained, using methods developed by Dr Gerald Siu, Columbia University, NY (personal communication). Briefly, cells (2×10⁶/ml) were suspended in phosphate-buffered saline (PBS), pH 7.2, with 3% fetal bovine serum (FBS). 1 ml suspension was centrifuged (1100 rpm, 5 minutes), the pellet was resuspended in 50 µl PBS with 3% FBS, then 1 ml ice-cold 80% ethanol was added and the suspension was incubated (4°C, 30 minutes). Fixed cells were centrifuged (1100 rpm, 5 minutes), and resuspended in 500 µl PBS containing 0.1 mg/ml propidium iodide and 0.6% NP-40. 500 µl PBS with 2 mg/ml RNaseA was added, the suspension was incubated in the dark (room temperature, 30 minutes), cells were resuspended, filtered through nylon mesh, and stored on ice until analysis in a FACSCalibur fluorescence-activated cell sorter (Becton-Dickinson, Mountain View, CA).

RESULTS

We prepared HeLa cells, HeLa-AS, which stably express an antisense RNA complementary to the 5' end of the human

MAP4 cDNA (nt64-386), containing the putative site of translational initiation (West et al., 1991). To prepare control cells, HeLa-S, we expressed the same sequence in sense orientation. To drive MAP4 antisense expression, we chose pCEP4 because it is constructed with Epstein-Barr virus elements, causing it to replicate within the host cell, maintain high copy number, and express extremely high levels of plasmid-encoded species (Belt et al., 1989; Cachianes et al., 1993). With expression vectors yielding weaker expression, we had previously been unsuccessful in significantly depleting endogenous MAP4, which is an abundant protein (0.1% of soluble protein in HeLa cells; Bulinski and Borisy, 1979). Moreover, since pCEP4 is maintained extra-chromosomally as an episome, rather than integrating into the genome, we could eliminate variability and artifacts due to point(s) of integration, when comparing transfected cell lines.

We determined that stably transfected clones expressed transfected MAP4 antisense sequences (in HeLa-AS cells) or the same sequence in sense orientation (in HeLa-S cells), using RT-PCR with one primer that lay within the vector sequence and one that lay within the antisense or sense cDNA fragment (Fig. 1). Next, we used western blots to determine that antisense expression yielded a significant reduction in MAP4 protein, relative to control cells, as shown in Fig. 2A. MAP4

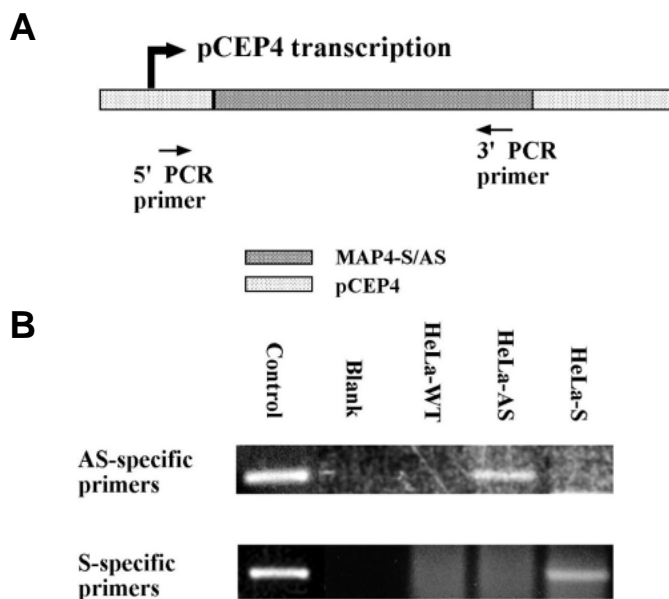


Fig. 1. HeLa-AS and HeLa-S cell lines express MAP4 antisense and sense transcripts. (A) Schematic diagram of PCR used to detect expression of sense and antisense MAP4 sequences. RT-PCR, using primers specific for MAP4 antisense or sense cDNAs, was used to detect expression of these sequences in HeLa-AS and HeLa-S cell lines. As shown, the 5' primer was designed to generate PCR product from any pCEP4-derived cDNA sequences, while the 3' primers corresponded to sequences specifically present in either MAP4 antisense or sense transcripts. (B) RT-PCR was performed with RNA from HeLa-WT, HeLa-AS and HeLa-S cells. Water rather than nucleic acid (Blank) was used as a negative control, and linearized pCEP4-MAP4-AS and pCEP4-MAP4-S were used as positive control PCR templates (Control). Note that MAP4-antisense cDNA was detected only in cDNAs from HeLa-AS cells and in the pCEP4-MAP4-AS control, while MAP4-sense cDNA was detected only in cDNA from HeLa-S cells and in the pCEP4-MAP4-S control.

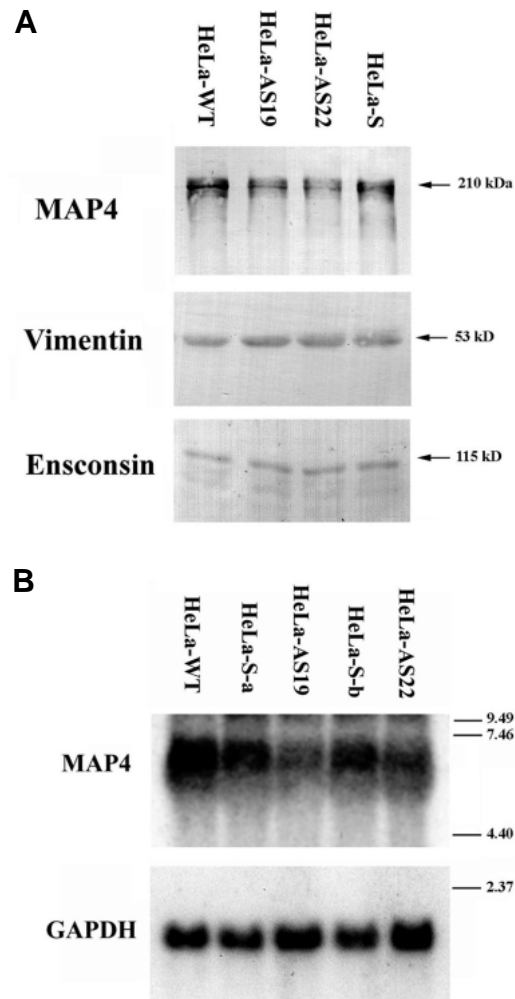


Fig. 2. HeLa-AS cells are decreased in MAP4 protein and mRNA transcripts. (A) Analysis of protein level. Samples of total cell extract (30 μ g protein per lane) from HeLa-WT, two clones of HeLa-AS (HeLa-AS19 and HeLa-AS22), and HeLa-S cells were electrophoresed, western-blotted onto nitrocellulose, and probed with anti-MAP4 and anti-vimentin antibodies. 40 μ g of protein from the same extracts were analyzed with anti-enscosin antibody (Bulinski and Bossler, 1994). Vimentin and enscosin levels were identical in HeLa-AS cells and controls. Mobilities of MAP4, vimentin and enscosin (210, 53 and 115 kDa, respectively) are noted, determined with electrophoretic mobility standards. (B) Analysis of mRNA transcript level. Northern blot of 20 μ g RNA from HeLa-WT, HeLa-AS19, HeLa-AS22 and two lines of HeLa-S, HeLa-S.a and HeLa-S.b., were probed for MAP4 transcripts and reprobed with a GAPDH probe, as a loading control. Note that MAP4 transcript level is lower in both HeLa-AS cell lines, compared to HeLa-WT and HeLa-S cells. Electrophoretic positions of 9.49, 7.46, 4.40 and 2.37 kb RNA markers are indicated.

level in HeLa-AS cells was depleted by as much as 70% relative to control cells, either untransfected HeLa (HeLa-WT) cells or HeLa-S cells. HeLa-AS cells contained, on average, 33.0% of the MAP4 level in HeLa-WT cells (Table 1A). For comparison, we measured vimentin levels; these were identical within experimental error in all lines, enabling us subsequently to use vimentin as a control (Fig. 2A). Since pCEP4 continuously replicates in the host cell, the number of vector

Table 1. Effects of MAP4 depletion on microtubule protein

| A | Cell line (<i>n</i>) | | |
|---|------------------------|-----------------|---------|
| | HeLa-AS‡ | HeLa-S‡ | HeLa-WT |
| Microtubule protein (% of WT) | | | |
| Amount of MAP4 (% of WT) | 33.03±2.95 (4) | 98.94±5.46 (4) | 100 (4) |
| Amount of total tubulin (% of WT) | 65.61±6.98 (5) | 96.60±10.86 (5) | 100 (5) |
| Tubulin synthesis* (% of WT) | 69.77±7.61 (2) | 100.74±1.21 (2) | 100 (2) |
| *Values are the amount of tubulin synthesized in 30 minutes, expressed relative to HeLa-WT. See Materials and Methods for details of procedures. All values are mean ± s.e.m. ‡Values are normalized relative to HeLa-WT. | | | |
| B | Cell line (<i>n</i>) | | |
| | HeLa-AS | HeLa-S | |
| Proportion of tubulin in polymer (% of total tubulin) | 59.39±1.16* (3) | 87.80±4.34* (4) | |
| Total MT polymer (% of control) | 45.94‡ | 100 | |
| % of tubulin in monomer | 40.61¶ | 12.2¶ | |
| Total tubulin monomer (% of control) | 226.1§ | 100 | |
| *Values are expressed as mean ± s.e.m. ‡Calculated from experimentally determined values, i.e. (% tubulin in polymer) × (amount of total tubulin, relative to HeLa-S control cells), and normalized to HeLa-S control cells. ¶Calculated from experimentally determined values, i.e. 100% – % tubulin in polymer. §Calculated as above for polymer and normalized to HeLa-S control cells. | | | |

copies per cell may vary, even within a clonal population. This continuous replication within the host cell ensures high-level expression from inserted cDNA and increases the likelihood that MAP4 level is uniformly depleted by the expressed antisense RNA in all cells. As shown in Fig. 2A, we detected no differences in extent of MAP4 depletion among HeLa-AS clonal lines. Although we verified each result with multiple HeLa-AS clones, only data for HeLa-AS22 are shown in all subsequent figures in this paper.

Since HeLa-AS cells are stable cell lines, we wondered if they might adapt to MAP4 depletion by upregulating other MAPs. The only other abundant MAP in HeLa cells, called E-MAP-115 or ensconsin (Masson and Kreis, 1993; Bulinski and Bossler, 1994), which is approximately as abundant as MAP4 (Bulinski and Borisy, 1979), has been shown to share with MAP4 a capacity to stabilize MTs in vitro or in transfected cells (Bulinski and Bossler, 1994; Masson and Kreis, 1993). As shown in Fig. 2A, the ensconsin level was not changed in HeLa-AS cells, suggesting that these cells do not respond to MAP4 depletion by increasing expression of another MAP that might be functionally similar to MAP4.

The decrease in MAP4 protein in HeLa-AS cells may be caused by degradation of MAP4 transcripts hybridized to antisense RNA, since ribonuclease that degrades double-stranded RNA is present in HeLa cells (Quesada et al., 1990). Instead, or in addition, antisense RNA could directly inhibit translation from MAP4 transcripts. To test whether transcript degradation contributed significantly to the decreased MAP4 level in HeLa-AS cells, we performed northern blots. As shown in Fig. 2B, MAP4 mRNA levels were lowered to a modest degree in HeLa-AS cells, as compared to control cells,

suggesting that MAP4 antisense transcript exerted its effect, in part, by inhibiting accumulation of MAP4 transcript.

The appearance of MTs and level of tubulin are altered in HeLa cells depleted of MAP4

A diminution in MAP4 staining and in the MT array of HeLa-AS cells was discernible by the qualitative technique of indirect immunofluorescence microscopy (Fig. 3). Although staining with MAP4 antibody was visible in both cell types (Fig. 3A,B), staining in HeLa-AS cells was only obvious in the thick, perinuclear region of the cells (Fig. 3A), while in HeLa-S cells MAP4 staining could be seen throughout the MT array, extending to the cell periphery (Fig. 3B). MAP4 immunofluorescence in all HeLa-AS cells looked similar, providing additional suggestive evidence that all cells were depleted in MAP4, and showing that any heterogeneity due to plasmid copy number in different cells was too insignificant to be detected.

The MT array of HeLa-AS cells (Fig. 3C) also appeared to be decreased in density, as compared to HeLa-S cells (Fig. 3D). Notably, the latter had bright foci of MTs emanating from their MTOCs, in contrast to HeLa-AS cells, which had diffuse staining near their nuclei and diminished focal arrays of MTs. The micrographs in Fig. 3C,D give the impression that brightness and quantity of out-of-focus fibers is greater in HeLa-S cells than in HeLa-AS cells (also see below for analysis of cell shape).

We confirmed this visual impression by biochemical measurements of tubulin and MT polymer in MAP4-depleted

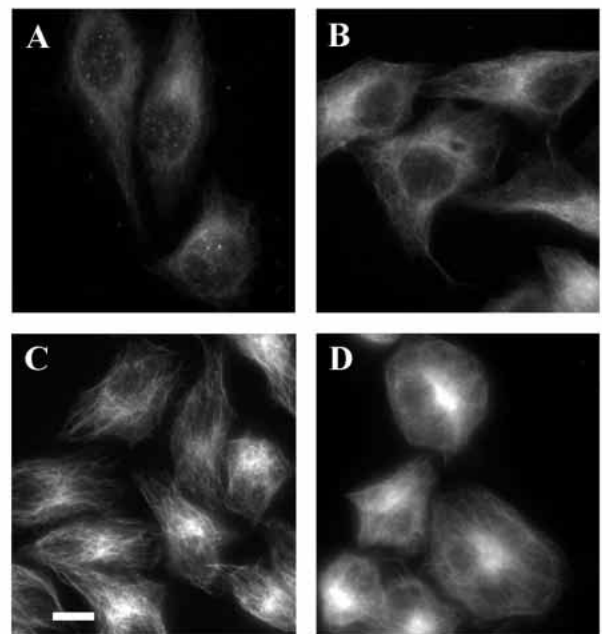


Fig. 3. HeLa-AS cells are diminished in levels of MAP4 and of MTs. Immunofluorescence images of HeLa-AS (A,C) and HeLa-S cells (B,D). Cells were stained with either anti-MAP4 (A,B) or anti-tubulin antibodies (C,D). Note that MAP4 staining of HeLa-AS cells, in A, is largely diffuse and appears dimmer than that of HeLa-S cells (B), although identical exposure times were used for A-D. Individual MTs in HeLa-AS cells (C) appear sharper than in HeLa-S cells (D). Bar, 10 μ m.

cells. Fig. 4 shows that HeLa-AS cells were decreased in their level of total tubulin, as compared to control cells. Quantification revealed that HeLa-AS cells possessed $65.6 \pm 7.0\%$ of the level of HeLa-WT cells, a result that was highly reproducible in four independent experiments (Table 1A). That cells with decreased levels of MAP4 also contained decreased levels of tubulin suggested that the steady state level of MT polymer assembled from this smaller tubulin pool might also be decreased.

Depletion of MAP4 alters monomer/polymer partitioning and synthesis of tubulin

Since MAP4 has been shown to promote *in vitro* MT polymerization by lowering the critical concentration (Aizawa et al., 1987), we reasoned that *in vivo* depletion of MAP4 might shift the equilibrium between polymer and protomer. Thus, we used a standard extraction protocol to fractionate cellular tubulin into polymeric and protomeric pools (see Materials and methods). Quantification of the proportion of tubulin in polymer in HeLa-AS and HeLa-S cells, as shown in Table 1B, demonstrates that, in addition to their decreased level of tubulin, the proportion of tubulin in polymer was also significantly decreased in HeLa-AS as compared to HeLa-S cells. For example, MAP4-depleted cells showed a mass of polymer only 45.9% that of control cells, and a proportion of tubulin in polymer that was 59.4% that of control cells. From these data, we calculated that the cytoplasmic protomer concentration in HeLa-AS cells was more than twice that in HeLa-S cells (Table 1B). Taken together, Fig. 4 and Table 1B demonstrate that depletion of MAP4 alters both content of MTs and partitioning of tubulin between polymeric and protomeric pools.

It has been proposed that tubulin protein synthesis is autoregulated by virtue of the fact that its synthesis was shown to be altered by acute changes in the cellular level of protomeric tubulin. For example, *increased* protomer, brought about by treating cells with MT-depolymerizing drugs (Ben-Ze'ev et al., 1979; Cleveland et al., 1981) or by microinjecting tubulin protomer into cells (Cleveland et al., 1981), resulted in dramatically *decreased* tubulin synthesis. Moreover, the converse result, that is, *decreased* protomer in cells treated with the MT-stabilizing drug, Taxol, yielded modestly *increased* tubulin synthesis (Cleveland et al., 1981; reviewed by

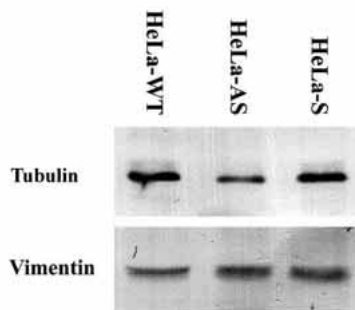


Fig. 4. Total tubulin level is decreased in MAP4-depleted cells. HeLa-WT, HeLa-AS and HeLa-S total cell extracts (6 μ g protein per lane) were electrophoresed, western-blotted and probed with anti-tubulin antibody, and restained with antibody against vimentin to verify protein loads. Positions of tubulin and vimentin are indicated.

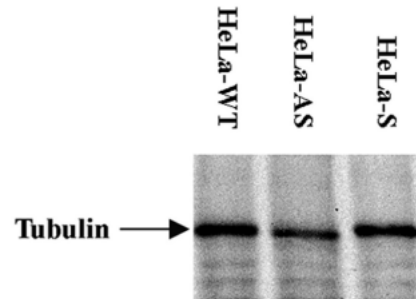


Fig. 5. Tubulin synthesis is decreased in MAP4-depleted cells. Tubulin was immunoprecipitated from an identical amount of TCA-precipitable counts of extract (i.e. 10^6 cpm TCA-precipitable 35 S-methionine) from HeLa-WT, HeLa-AS and HeLa-S cells, electrophoresed and autoradiographed, showing that HeLa-AS cells synthesized less tubulin during the 30-minute pulse-labeling period than did control cells. The electrophoretic position of tubulin is indicated in the autoradiogram.

Cleveland and Theodorakis, 1994). Since MAP4 depletion alters partitioning between protomeric and polymeric tubulin pools, such that cells have an increased concentration of protomer (Table 1B), we tested the hypothesis that MAP4 depletion might impact upon tubulin synthesis.

We analyzed tubulin synthesis in HeLa-AS cells by methods identical to those of Cleveland et al. (1981). As shown in Fig. 5, we found that the amount of tubulin synthesized during the standard 30-minute pulse label (Cleveland et al., 1981), was decreased in HeLa-AS cells, as compared to either HeLa-S or HeLa-WT cells. This decrease was similar in magnitude to the decrease in steady-state tubulin level in the same cells (Table 1A), demonstrating that the altered tubulin level in HeLa-AS cells could arise from altered tubulin synthesis. As an experimental control, we measured total protein synthesis, that is, incorporation of label into total TCA-precipitable protein. Total protein synthesis was not altered by MAP4 depletion (data not shown), demonstrating that MAP4 antisense specifically inhibited tubulin synthesis, rather than nonspecifically inhibiting total protein synthesis.

To postulate that MAP4 affects tubulin synthesis because it alters tubulin protomer level, we needed to establish that HeLa cells exhibit this autoregulatory mechanism, since tubulin synthesis had not been studied previously in HeLa cells. Accordingly, we treated HeLa-WT cells with nocodazole and Taxol, which yielded greatly decreased and modestly increased tubulin synthesis, respectively, as predicted from the model (data not shown). Thus, our results are consistent with the hypothesis that increased steady-state level of tubulin protomer, caused by depletion of MAP4's MT-stabilization activity, impacts upon tubulin's autoregulatory machinery and decreases translation of tubulin in HeLa-AS cells.

MAP4-depleted cells can be rescued by reexpression of MAP4 MT-binding domain

To demonstrate that the effects we measured in HeLa-AS cells were attributable to depletion of MAP4, rather than to non-specific effects of antisense expression, we attempted to 'rescue' MAP4-depleted cells by retransfecting them with a vector encoding the MT-binding domain (MTB) of MAP4. We chose MTB because, like full-length MAP4, it can stabilize

MTs in vitro (Aizawa et al., 1991) and in vivo (Olsen et al., 1995; Yoshida, 1996; Nguyen et al., 1997). To detect MTB in re-transfected cells, we attached a GFP-encoding moiety to the 5' end of MTB-coding sequence. Since MTB is encoded in the 3' one-third of MAP4-coding sequence, while the antisense sequence corresponds to the far 5' end of MAP4 cDNA, the GFP-MTB rescue construct would be incapable of hybridizing with, or being inhibited in expression by, the antisense construct already expressed in HeLa-AS cells.

As the simplest and most direct assay for phenotypic rescue of HeLa-AS cells, we measured tubulin levels. Fig. 6 shows that expression of GFP-MTB was detectable in HeLa-AS cells, and that its expression was sufficient to restore tubulin content of HeLa-AS cells to at least wild-type levels. In fact, in the experiment shown, tubulin content was increased to a level even greater than that of wild-type cells. Ability to rescue HeLa-AS cells by expressing GFP-MTB supports our contention that changes in the MTs in HeLa-AS cells were truly caused by expression of MAP4-antisense sequences and consequent depletion of intracellular MAP4. Furthermore, these findings strongly support the hypothesis that the MAP4 level directly influences tubulin level, since, in the same cell system, lowering (HeLa-AS cells) or raising (HeLa-AS-rescue cells) MAP4 levels manipulated tubulin levels in opposite directions.

MT polymerization is compromised in MAP4-depleted cells

Previous studies showed that overexpression of MAP4

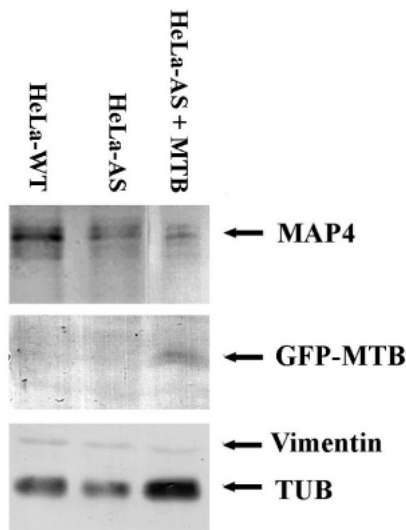


Fig. 6. Rescue of MAP4-depleted cells by transfection of MAP4 MT-binding domain. HeLa-AS cells were transfected with a vector expressing a chimera of GFP and MAP4 MT-binding domain (GFP-MTB). Western blotting of extracts of equal quantities of MAP4-depleted (HeLa-AS), wild-type (HeLa-WT) and HeLa-AS cells expressing GFP-MTB (HeLa-AS+MTB) were immunolabeled with anti-tubulin antibodies to assay tubulin content. HeLa-AS+MTB showed an increased level of tubulin relative to HeLa-AS cells; note that a comparison of the tubulin band in the HeLa-AS+MTB lane to that in the HeLa-WT lane reveals that in the experiment shown, transfection of GFP-MTB into HeLa-AS cells increased the tubulin content of the MAP4-depleted cells to a level greater than the wild-type tubulin level. Electrophoretic positions of MAP4, GFP-MTB, vimentin and tubulin are indicated.

increased stability or longevity of MTs (Olsen et al., 1995; Nguyen et al., 1997), while steady-state measurements of MAP4-depleted cells showed diminished MT polymer levels. These two observations prompted us to hypothesize that tubulin polymerization might be less efficient in MAP4-depleted cells than in cells containing a wild-type level of MAP4. To test this hypothesis, we examined HeLa-AS and HeLa-S cells whose MTs were allowed to repolymerize after complete depolymerization by nocodazole. In both cell types, nocodazole depolymerized all MTs (not shown). After drug removal, MTs repolymerized in two distinct phases. In the first phase, observed 1 minute after drug removal (T=1 minute), small MT asters formed at the centrosome. In the second, observed at T=2 minutes, long MTs were formed. In the second phase, cells were heterogeneous in their patterns of MT reformation. Many cells displayed an astrally focused pattern; that is, their long MTs appeared to originate from one or more centrosomes. Other cells exhibited unfocused regrowth; their MTs were usually shorter and they appeared to initiate from multiple sites throughout the cytoplasm. The micrographs in Fig. 7 document the progress of MT polymerization in HeLa-AS and HeLa-S control cells, with examples of cells in each phase of regrowth, at T=1 minute (Fig. 7A,B) and T=2 minutes (Fig. 7C,D). In both cell types, asters initiated MT formation; however, both speed of regrowth and extent to which the

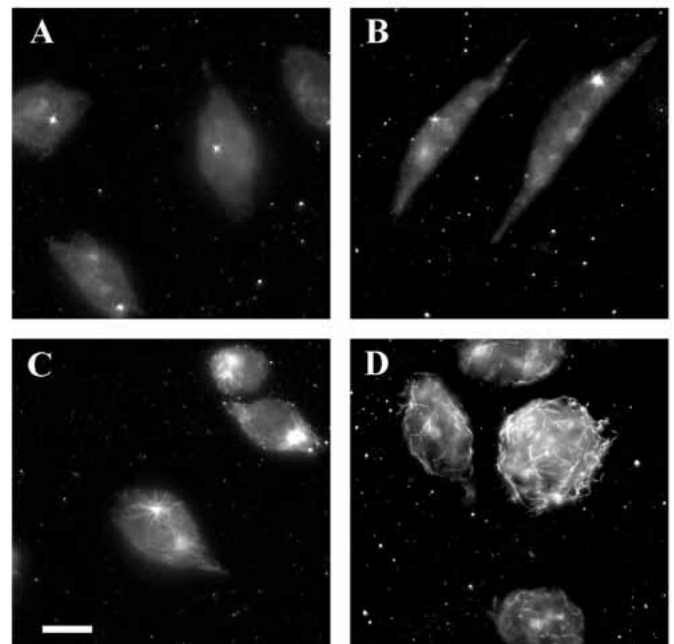


Fig. 7. Altered pattern of in vivo MT polymerization in HeLa-AS cells. Micrographs show HeLa-AS (A,C) and HeLa-S (B,D) cells treated with 15 μ M nocodazole for 2 hours to depolymerize all MTs, then released into drug-free medium for 1 minute (A,B) or 2 minutes (C,D) to allow MT regrowth. Before methanol fixation and immunofluorescence staining with anti-tubulin antibodies, cells were extracted with 200 μ g/ml saponin (37°C, 2 minutes) to remove protomeric tubulin. Note that astral MTs appear shorter in A than in B. MTs in the HeLa-AS cells (C) also appear to have regrown in a more astrally focused pattern than those shown in the HeLa-S cells (D). See Table 2 for quantitative analysis of these experiments. Bar, 10 μ m.

forming array was focused on the centrosome differed between HeLa-AS and HeLa-S cells.

We performed quantitative analysis of regrowth in the two cell types, as shown in Table 2. Taken together, data in Fig. 7 and Table 2 demonstrate that, after release from drug-induced depolymerization, MTs in HeLa-AS cells reformed more slowly than in HeLa-S cells. For example, asters in HeLa-AS cells at T=1 minute were smaller than those in HeLa-S cells (Fig. 7A,B), and there was twice the percentage of cells devoid of MTs at this time point in HeLa-AS cells (20.7%) as in HeLa-S cells (40.4%). The difference in speed of MT regrowth was even more striking at T=2 minutes: virtually all HeLa-S cells had entered the second phase of MT regrowth (98.4%), while about one-third of HeLa-AS cells (35.3%) either had not commenced MT regrowth at all, or had formed only small asters. The fact that MAP4 depletion decreased rate of MT regrowth suggests that MAP4 influences MT polymerization rate. This could occur directly, due to MAP4 stabilizing MT polymers as they form, as has been documented in vitro (Aizawa et al., 1991). Alternatively, MAP4 could influence MT polymerization rate indirectly by raising the cell's tubulin level. MT polymerization rate has been shown to be roughly proportional to the concentration of tubulin protomers (Walker et al., 1988).

Not only speed, but also pattern, of MT regrowth differed between HeLa-AS and HeLa-S cells. At T=2 minutes, about half of the HeLa-AS cells (47.9%) had polymerized MTs from the centrosome in an astrally focused pattern (Fig. 7C). In contrast, at this time point a much greater proportion of HeLa-S cells (78.1%) had repolymerized MTs in an unfocused pattern in which most MTs could not be traced back to centrosomal sites (Fig. 7D). Regrowth was essentially complete in both cell types at T=10 minutes. Moreover, MT organization was indistinguishable in the two cell types after full recovery from drug; MTs filled the cells, and most could be traced back to origins at the centrosome (data not shown). Differences in the pattern of regrowth raise the possibility that MAP4 may nucleate MTs. Alternatively, or in addition, MAP4 may function indirectly: by raising the cellular tubulin level, MAP4 may promote spontaneous MT nucleation, which requires a threshold concentration of protomer (Timasheff and Grisham, 1980).

Depletion of MAP4 yields morphological changes in HeLa cells

Next, we asked whether MAP4 depletion caused any changes

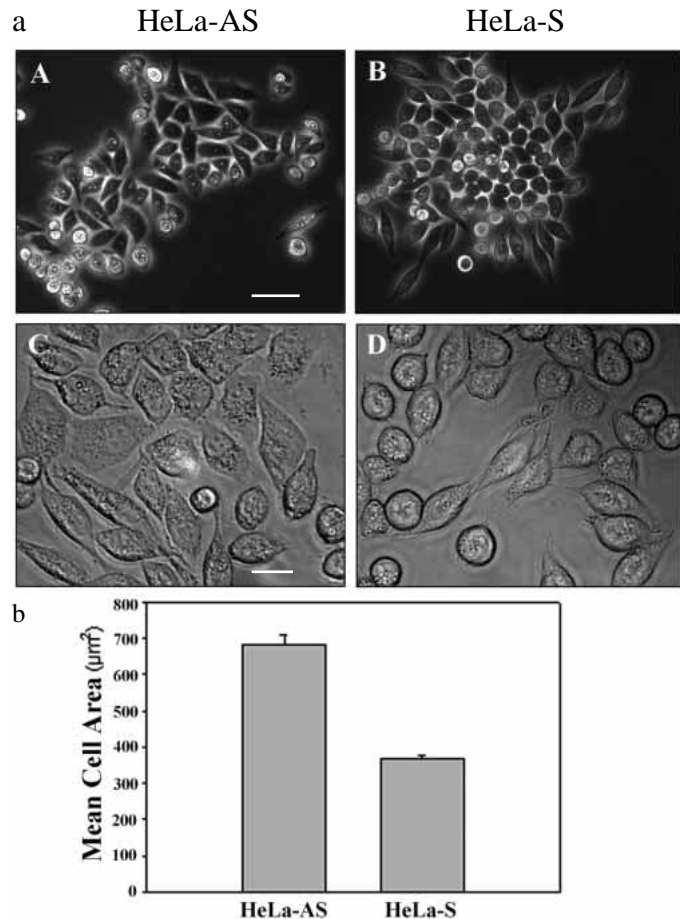


Fig. 8. (a) Altered morphology of MAP4-depleted cells. Phase contrast micrographs of HeLa-AS (A,C) and HeLa-S (B,D) cells visualized at 60 \times (A,B) and 250 \times (C,D) magnifications. Note the larger area and flatter appearance of HeLa-AS cells, as compared to HeLa-S cells. Bars, 50 μ m (A); 10 μ m (C). (b) HeLa-AS cells spread over a significantly larger area than HeLa-S cells. Surface areas of HeLa-AS and HeLa-S cells were determined as described in Materials and methods. Values are mean \pm s.e.m.

in cell morphology. When cultured in hygromycin, both HeLa-AS and HeLa-S cells assumed a subtly different, flatter appearance than HeLa-WT cells (data not shown). Thus, to avoid potential artifacts, we compared the morphologies of HeLa-AS and HeLa-S cells in the presence of the selecting

Table 2. Effects of MAP4 depletion on MT regrowth

| Patterns of MT regrowth after release from nocodazole depolymerization | | | | | |
|--|---------------|-------------|------------------------------|---------------------------------------|-------------------------------------|
| Time after release (minutes) | Cell line (n) | No MTs* (%) | Tiny asters [‡] (%) | Astrally focused MTs [§] (%) | Unfocused disarray [¶] (%) |
| 0 | HeLa-AS (112) | 100 | 0 | 0 | 0 |
| | HeLa-S (114) | 100 | 0 | 0 | 0 |
| 1 | HeLa-AS (104) | 40.4 | 59.6 | 0 | 0 |
| | HeLa-S (116) | 20.7 | 66.4 | 0 | 12.9 |
| 2 | HeLa-AS (143) | 9.2 | 26.1 | 47.9 | 16.9 |
| | HeLa-S (128) | 0 | 1.6 | 20.3 | 78.1 |

Values are expressed as a percentage of total number of cells scored.

*No microtubules visible by immunofluorescence microscopy. See Materials and Methods for details on microscopy.

[‡]Small asters were visible as a bright dot with no significant microtubule growth.

[§]Significant MT growth, originating primarily from one or more centrosomes.

[¶]Significant microtubule growth in a disorderly pattern, with no significant focus on one or more centrosomes.

drug, hygromycin. We noted qualitative differences in morphology; HeLa-AS cells appeared to be less bipolar, and they were flatter and better spread than HeLa-S cells (Fig. 8a). To compare cell morphology quantitatively, we measured the surface area of spread cells. Fig. 8b shows that HeLa-AS cells spread over a significantly larger area than HeLa-S cells, confirming our qualitative visual assessment. We noted that HeLa-AS cells were more heterogeneous in surface area than HeLa-S cells (data not shown). This could be a significant finding; however, we could not rule out the possibility that heterogeneity was due to variable numbers of vector copies and, hence, variegated MAP4 level in individual HeLa-AS cells. We determined that cell volume, as measured by FACS, was identical for the two cell types, verifying that HeLa-AS cells were actually flatter, that is, less tall, than control cells. These results suggest that MAP4 functions in determination of cell morphology, either directly or indirectly, through its modulation of MT level.

DISCUSSION

When we embarked upon this study, there was abundant evidence suggesting that MAP4 could regulate the assembly-state of intracellular tubulin. For example, *in vitro* experiments had shown that MAP4 lowered the critical concentration of tubulin required for assembly and increased the mass of MTs assembled (Aizawa et al., 1987, 1991). Likewise, *in vivo* experiments had shown that increasing the intracellular level of MAP4 increased stability and longevity of MTs (Olsen et al., 1995; Yoshida et al., 1996; Nguyen et al., 1997). However, apparently contradictory results had been reported by Wang et al. (1996). These investigators microinjected cells with anti-MAP4 antibodies designed to ablate MAP4's MT-binding ability; they observed no effect on turnover of the MT population, as measured by a dual fluorochrome technique. From their results, Wang et al. suggested that MAP4 either does not play a role in stabilizing MTs *in vivo* or that MAP4's role is redundant with that of other molecules. We decided to address the disparity in results by studying populations of HeLa cells deficient in MAP4, in which we could quantitatively assess the role(s) of MAP4 in regulating the MT system.

Our results show that MAP4 indeed exerts profound effects on the MT system. MAP4 depletion resulted in lowered intracellular tubulin level (Fig. 4; Table 1A), and decreased level and proportion of tubulin present as assembled MTs (Table 1B). In contrast to the study of Wang et al. (1996), whose single-cell microinjection technique precluded biochemical analyses of quantitative effects on MTs caused by depletion of active MAP4, our anti-sense results allowed us to measure the phenotypic contributions of MAP4.

Results of these anti-sense studies suggest that MAP4 plays a central role in regulating intracellular level of tubulin and MTs, a role that apparently cannot be supplanted by other proteins present in HeLa cells. These results are significant in light of results demonstrating that proper allocation of tubulin between monomeric and polymeric states is important for the successful performance of a variety of cell activities. For example, during development, establishment of dorsoventral polarity in *Xenopus laevis* embryos involves a shift in the

cytoplasm relative to the cortex. This shift is temporally correlated with a transient increase in the level of polymeric tubulin (Elinson, 1985), and this process has been shown to be disrupted by MT depolymerizing drugs (Scharf and Gerhart, 1983; Elinson, 1983).

In a similar vein, recent studies of myocardial hypertrophy resulting from pressure overload of cardiac tissue have suggested that changes in levels of both MTs and of MAP4 are physiologically significant. For example, an increased MT polymer level has been observed in cardiomyocytes during hypertrophy and appears to play a key role in contractile dysfunction of cardiocytes (Tsutsui et al., 1993, 1994). Sato et al. (1997) found that levels of both MAP4 transcript and protein were elevated at stages *before* increased MT numbers were detected. Coupled with data demonstrating that MAP4 regulates MT levels, this temporal correlation supports the notion that MAP4 is involved in modulating the assembly state and level of MTs in cardiac hypertrophy.

Our data corroborate the observations of Esmaeli-Azad et al. (1994), that PC12 cells transfected with a tau antisense construct exhibited lowered MT levels and reduced rate of neurite outgrowth. The congruity between their results and ours is not surprising, considering that the MT-binding domains of the two MAPs are homologous. These results raise the possibility that tau and MAP4 could functionally compensate for each other, to some degree. We note that HeLa cells do not express tau or other homologous MAPs. In contrast, the fact that tau and MAP4 are functionally similar clouds the interpretation of experiments in which a tau-null mouse was generated and partially characterized (Harada et al., 1994). In these mice, the possibility that MAP4 may compensate for loss of tau function has not been addressed. Since tau and MAP2 are not expressed in HeLa, it is unlikely that other MAPs compensate for depletion of MAP4 function in HeLa-AS cells; any compensation that occurred would have lessened the phenotypic abnormalities we measured. Expression of the only other MAP known to be abundant in HeLa cells, enscosin (Masson and Kreis, 1993; Bulinski and Bossler, 1994), was not changed in HeLa-AS cells.

We determined that the cellular level of tubulin protomer at steady state was increased in MAP4-depleted cells; we noted a concomitant decrease in tubulin synthesis that was similar in magnitude to the decrease in tubulin (Figs 4,5, Table 1). The mechanism most consistent with these data is that MAP4 promotes MT assembly and this affects tubulin synthesis by the mechanism shown in Fig. 9 (developed from our data and the model of Cleveland et al., 1981). The autoregulation portion of this model is supported by experiments in which the tubulin protomer level was transiently elevated, and tubulin synthesis decreased (Ben-Ze'ev et al., 1979; Caron et al., 1985; Pittenger and Cleveland, 1985). It is also supported by our data on the consequences of MAP4 depletion. Further support for this model stems from results of the rescue experiment; introduction of the GFP-MTB chimera restored the tubulin level of MAP4-depleted cells to at least the wild-type level. Finally, the model is corroborated by previous work: cells exhibiting high-level overexpression of partial- or full-length MAP4 exhibited an increased steady-state tubulin level (L-MAP4-#13-2 and L-MTB#3-6 lines; Nguyen et al., 1997). Together, results in which elevation or depletion of MAP4 increase or decrease tubulin level, respectively, provide strong

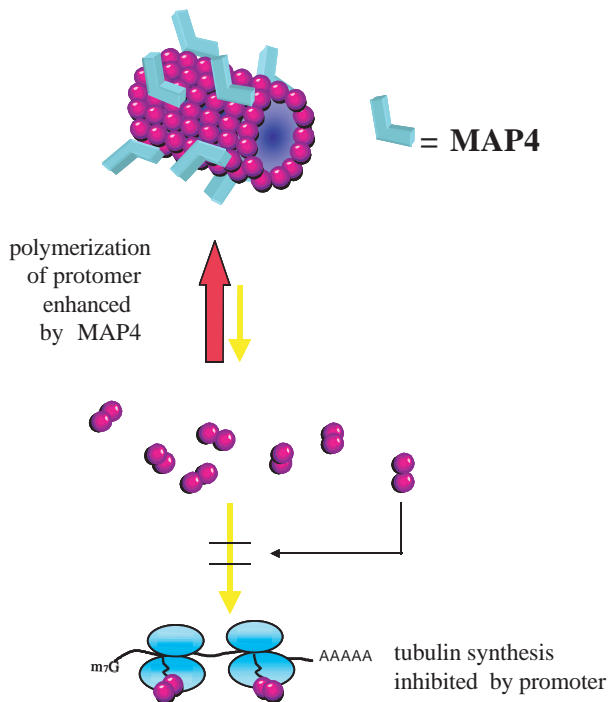


Fig. 9. Model for MAP4's role in regulating tubulin and MT levels. According to this model, MAP4 stabilizes MTs and promotes their polymerization, thus decreasing the level of protomeric tubulin. In addition, since protomeric tubulin inhibits its own synthesis, stabilization of MTs by MAP4 decreases the concentration of protomeric tubulin, yielding greater tubulin synthesis and increasing the steady-state level of tubulin. This model is based upon data presented in this paper for HeLa-AS cells, including the increased proportion and amount of protomeric tubulin, the decreased synthesis and steady-state level of tubulin, and the lower rate and extent of MT polymerization exhibited by these cells. The model shown has as its genesis that originally proposed by Cleveland et al. (1981).

support for the hypothesis that MAP4 stabilizes the polymeric state of tubulin and impacts on the steady-state level of tubulin through the tubulin autoregulation mechanism.

In systems containing pure tubulin, the dynamic instability model predicts that the concentration of polymer will be proportional to that of protomer (Mitchison and Kirschner, 1984). Alteration in the levels of tubulin partitioned into protomer and polymer in HeLa-AS and HeLa-S cells indicated that MAP4 depletion decreased the proportion of tubulin in polymer and increased the fraction in protomer. Thus, tubulin protomer concentration, alone, cannot account for the level of MTs *in vivo*; instead, data presented here suggest that MAP4 plays a major role in determining MT level *in vivo*, as depicted in Fig. 9. The demonstration that an assembly-promoting MAP, MAP4, impacts upon tubulin protomer-polymer partitioning provides a more complete picture of the factors regulating the dynamic equilibrium between tubulin protomer and polymer in living cells.

Additional methods by which MAP4 regulates the MT system are suggested by the results of MT regrowth experiments. HeLa-AS cells were slower in reforming their MT network after release from drug depolymerization, and they were impaired in their ability to nucleate non-centrosomal

MTs (Fig. 7, Table 2). These results are consistent with two *in vitro* results. First, MAPs such as MAP4 increase the rate of MT growth and lower the critical concentration necessary for spontaneous polymerization, by stabilizing polymers (Bulinski and Borisy, 1980a; Aizawa et al., 1991). MT regrowth results suggest that MAP4 accelerates polymerization of MTs, including MTs not associated with the centrosome, by stabilizing newly formed MTs. Second, *in vitro* polymerization of MTs occurs more rapidly at higher tubulin concentrations, and spontaneous (non-nucleated) polymerization occurs only at tubulin concentrations exceeding the critical concentration for prevailing conditions (Timasheff and Grisham, 1980). Thus, MAP4 may accelerate polymer formation and promote formation of non-centrosomal MTs merely by raising the concentration of tubulin above the critical concentration that obtains in cytoplasm. Results on MT regrowth suggest that, either directly, indirectly or both, MAP4 hastens MT polymerization and promotes nucleation of MTs *in vivo*.

In undifferentiated carcinoma cells, such as HeLa, MTs only undergo complete regrowth of their cytoplasmic array following cell division. Moreover, interphase MTs in HeLa cells are organized in a radial pattern originating primarily from the MT organizing center (MTOC); defects in nucleation of non-centrosomally associated MTs would be unlikely to compromise this array significantly. The existence of non-centrosomal MTs at steady-state has not been demonstrated in HeLa cells, which have such a small cytoplasmic volume that MTs can span the distance from attachment points at the MTOC to the cell periphery. However, in other undifferentiated epithelial cells, PtK₁ and A498 cells, Vorobjev et al. (1997) and Yvon and Wadsworth (1997) demonstrated the existence of a significant group of MTs not attached to MTOC sites. Vorobjev et al. (1997) determined that, in PtK₁ cells, non-centrosomal MTs most likely formed *de novo*, rather than arising from MTs originally nucleated by MTOCs.

Although the role of MTs not attached to the MTOC is not known in undifferentiated cells such as PtK₁ and A498, non-MTOC MTs comprise the major population in certain differentiated cells, notably neurons (Baas and Black, 1991) and polarized epithelia (Bré et al., 1987). Non-MTOC MTs are necessarily important in differentiated neurons, myotubes and epithelia, whose asymmetry and size preclude extension of MTs from the MTOC to the cell periphery. Thus, MAP4's role in nucleating or stabilizing non-MTOC MTs may be most important in differentiated cells.

Despite the fact that they were not devoid of MAP4, HeLa-AS cells displayed obvious morphological abnormalities. For example, they spread over a larger surface area. This result suggests that MAP4 is involved in regulation of cell shape. This is the only evidence to date of such a role for the major, ubiquitously expressed form of MAP4. However, this result is reminiscent of results obtained with other MAPs. For example, depletion of either MAP2 or tau impaired the ability of neuronal cells to differentiate and extend neurites (Caceres and Kosik, 1990; Dinsmore and Solomon, 1991). In addition, inhibition of a specialized, muscle-specific isoform of MAP4 in C₂C₁₂ myoblasts was reported to lead to aberrant myogenesis (Mangan et al., 1996). This last result, combined with our current data, suggest that, in non-neuronal cells, MAP4 plays a role analogous to roles tau and MAP2 play in neuronal cells. Alternatively, morphological effects we

observed here – as well as those reported for other MAPs – may be caused indirectly by the decreased level of MTs in MAP-depleted cells. Taken together, our results with MAP4 and those with other MAPs demonstrate that cells necessarily regulate their level of MAPs and MTs to control their shape.

Our results with cells in which MAP4 has been depleted to about one-third of the wild-type level establish that MAP4 imbues cellular MTs with properties neither observed nor even modeled for MTs composed of tubulin alone (Mitchison and Kirschner, 1984, 1987). Our data show that MAP4 influences the MT array of non-neuronal cells, not only by modulating the level of tubulin and MTs, but also by affecting the level of non-centrosomal MTs, and it also impacts upon other cellular functions, like cell spreading. Our findings raise the possibility that a more complete ablation of MAP4, for example, via genetic knockout, may yield intriguing phenotypes. These phenotypes may lend insight into functions of MAPs and of MTs in complex cellular processes, such as development and morphogenesis.

The authors are grateful to Drs Ghassan Samara, Michael Sheetz, Ted Salmon, Gary Borisy, Clare Waterman-Storer and George Cooper for invigorating discussions. This research was supported by the National Institutes of Health, a grant (CA-70951) to J. C. B. and a predoctoral traineeship (T32-CA09503) to H. L. N.

REFERENCES

- Aizawa, H., Murofushi, H., Kotani, S., Hisanaga, S.-I., Hirokawa, N. and Sakai, H. (1987). Limited chymotryptic digestion of bovine adrenal 190,000-Mr microtubule-associated protein and preparation of a 27,000-Mr fragment which stimulates microtubule assembly. *J. Biol. Chem.* **262**, 3782-3787.
- Aizawa, H., Emori, Y., Mori, A., Murofushi, H., Sakai, H. and Suzuki, K. (1991). Functional analysis of the domain structure of MT-associated protein 4 (MAP4). *J. Biol. Chem.* **266**, 9841-9846.
- Baas, P. W. and Black, M. M. (1990). Individual microtubules in the axon consist of domains that differ in both composition and stability. *J. Cell Biol.* **111**, 495-509.
- Belt, P. G. B. M., Groeneveld, H., Teubel, W. J., van de Putte, P. and Backendorf, C. (1989). Construction and properties of an Epstein-Barr-virus-derived cDNA expression vector for human cells. *Gene* **84**, 407-417.
- Ben-Ze'ev, A., Farmer, S. R. and Penman, S. (1979). Mechanisms of regulating tubulin synthesis in cultured mammalian cells. *Cell* **17**, 319-325.
- Bré, M.-H., Kreis, T. E. and Karsenti, E. (1987). Control of MT nucleation and stability in Madin-Darby canine kidney cells: the occurrence of noncentrosomal, stable MTs. *J. Cell Biol.* **105**, 1283-1296.
- Bulinski, J. C. (1994). MAP 4. In *Microtubules* (ed. J. Hyams and C. W. Lloyd), pp. 167-182. New York: Wiley & Sons.
- Bulinski, J. C. and Borisy, G. G. (1979). Self-assembly of HeLa tubulin and the identification of HeLa microtubule-associated proteins. *Proc. Natl. Acad. Sci. USA* **76**, 293-297.
- Bulinski, J. C. and Borisy, G. G. (1980a). Microtubule-associated proteins from cultured HeLa cells: Analysis of molecular properties and effects on MT polymerization. *J. Biol. Chem.* **255**, 11570-11576.
- Bulinski, J. C. and Borisy, G. G. (1980b). Widespread distribution of a 210,000 mol wt microtubule-associated protein in cells and tissues of primates. *J. Cell Biol.* **87**, 802-808.
- Bulinski, J. C. and Bossler, A. B. (1994). Purification and characterization of enscosin, a novel microtubule-stabilizing protein. *J. Cell Sci.* **107**, 2839-2849.
- Caceres, A. and Kosik, K. S. (1990). Inhibition of neurite polarity by antisense oligonucleotides in primary cerebellar neurons. *Nature* **343**, 461-463.
- Cachianes, G., Ho, C., Weber, R. F., Williams, S. R., Goeddel, D. V. and Leung, D. W. (1993). Epstein-Barr virus-derived vectors for transient and stable expression of recombinant proteins. *BioTechniques* **15**, 255-258.
- Caron, J. M., Jones, A. L., Ball, L. B. and Kirschner, M. W. (1985). Autoregulation of tubulin synthesis in enucleated cells. *Nature* **317**, 648-651.
- Chapin, S. and Bulinski, J. C. (1991a). Non-neuronal 210 kD MT-associated protein (MAP4) contains a domain homologous to the MT-binding domains of MAP2 and tau. *J. Cell Sci.* **98**, 27-36.
- Chapin, S. J. and Bulinski, J. C. (1991b). Preparation and functional assay of tyrosinated and detyrosinated tubulin. *Meth. Enzymol.* **196**, 254-264.
- Chapin, S., Lue, C.-M., Yu, M. T. and Bulinski, J. C. (1995). Differential expression of alternatively spliced forms of MAP4: A repertoire of structurally different MT-binding domains. *Biochemistry* **34**, 2289-2301.
- Cleveland, D. W., Lopata, M. A., Sherline, P. and Kirschner, M. W. (1981). Unpolymerized tubulin modulates the level of tubulin mRNAs. *Cell* **25**, 537-546.
- Cleveland, D. W. and Theodorakis, N. G. (1994). Regulation of tubulin synthesis. In *Microtubules* (ed. J. Hyams and C. W. Lloyd), pp. 47-58. New York: Wiley & Sons.
- Dinsmore, J. H. and Solomon, F. (1991). Inhibition of MAP2 expression affects both morphological and cell division phenotypes of neuronal differentiation. *Cell* **64**, 817-826.
- Elinson, R. P. (1983). Cytoplasmic phases in the first cell cycle of the activated frog egg. *Dev. Biol.* **100**, 440-450.
- Elinson, R. P. (1985). Changes in the levels of polymeric tubulin associated with activation and dorsoventral polarization of the frog egg. *Dev. Biol.* **109**, 224-233.
- Esmaili-Azad, B., McCarty, J. H. and Feinstein, S. C. (1994). Sense and antisense transfection analysis of tau function: tau influences net microtubule assembly, neurite outgrowth and neuritic stability. *J. Cell Sci.* **107**, 869-879.
- Faruki, S. and Karsenti, E. (1994). Purification of microtubule proteins from *Xenopus* egg extracts: identification of a 230K MAP4-like protein. *Cell Motil. Cytoskel.* **28**, 108-118.
- Goedert, M., Baur, C. P., Ahninger, J., Jakes, R., Hasegawa, M., Spillantini, M. G., Smith, M. J. and Hill, F. (1996). PTL-1 a microtubule-associated protein with tau-like repeats from the nematode *Caenorhabditis elegans*. *J. Cell Sci.* **109**, 2661-2672.
- Gundersen, G. G., Khawaja, S. and Bulinski, J. C. (1987). Post-polymerization detyrosination of alpha tubulin: A mechanism for subcellular differentiation of microtubules. *J. Cell Biol.* **105**, 251-264.
- Harada, A., Oguchi, K., Okabe, S., Kuno, J., Terada, S., Ohshima, T., Sato-Yoshitake, R., Takei, Y., Noda, T. and Hirokawa, N. (1994). Altered MT organization in small-calibre axons of mice lacking tau protein. *Nature* **369**, 488-491.
- Huber, G. and Matus, A. (1990). MT-associated protein 3 (MAP3) expression in non-neuronal tissues. *J. Cell Sci.* **95**, 237-246.
- Itoh, T. J. and Hotani, H. (1994). MT-stabilizing activity of MT-associated proteins (MAPs) is due to increase in frequency of rescue in dynamic instability: shortening length decreases with binding of MAPs onto microtubules. *Cell Struct. Funct.* **19**, 279-290.
- Kroczek, R. A. and Siebert, E. (1990). Optimization of northern analysis by vacuum-blotting, RNA-transfer visualization and ultraviolet fixation. *Anal. Biochem.* **184**, 90-5.
- Mandelkow, E. and Mandelkow, E. M. (1995). Microtubules and microtubule-associated proteins. *Curr. Opin. Cell Biol.* **7**, 72-81.
- Mangan, M. E. and Olmsted, J. B. (1996). A muscle-specific variant of microtubule-associated protein 4 (MAP4) is required in myogenesis. *Development* **122**, 771-781.
- Masson, D. and Kreis, T. E. (1993). Identification and molecular characterization of E-MAP-115, a novel microtubule-associated protein predominantly expressed in epithelial cells. *J. Cell Biol.* **123**, 357-371.
- McDermott, J. B., Aamodt, S. and Aamodt, E. (1996). pti-1, a *Caenorhabditis elegans* gene whose products are homologous to the tau microtubule-associated proteins. *Biochemistry* **35**, 9415-23.
- Mitchison, T. J. and Kirschner, M. W. (1984). Dynamic instability in MT growth. *Nature* **312**, 237-242.
- Nguyen, H. L., Chari, S., Lue, C.-M., Gruber, D., Chapin, S. and Bulinski, J. C. (1997). Overexpression of full- or partial-length MAP4 stabilizes MTs and alters cell growth. *J. Cell Sci.* **110**, 281-294.
- Olsen, K. R., McIntosh, J. R. and Olmsted, J. B. (1995). Analysis of MAP4 function in living cells using green fluorescent protein (GFP) chimeras. *J. Cell Biol.* **130**, 639-650.
- Oosawa, F. and Asakura, S. (1975). *Thermodynamics of the Polymerisation of Protein*. London: Academic Press.
- Parysek, L. M., Asnes, C. F. and Olmsted, J. B. (1984). MAP4: occurrence in mouse tissues. *J. Cell Biol.* **99**, 1309-1315.

- Pittenger, M. F. and Cleveland, D. W.** (1985). Retention of autoregulatory control of tubulin synthesis in cytoplasts: Demonstration of a cytoplasmic mechanism that regulates the level of tubulin expression. *J. Cell Biol.* **101**, 1941-1952.
- Quesada, P. Merola, M., Farina, B. and Leone, E.** (1990). In vitro inhibition of HeLa cell nuclear ribonucleases by ADP ribosylation. *Mol. Cell. Biochem.* **94**, 53-60.
- Sambrook, J., Fritsch, E. F. and Maniatis, T.** (1989). *Molecular Cloning: A Laboratory Manual*, 2nd edition. New York: Cold Spring Harbor Laboratory Press.
- Scharf, S. R. and Gerhart, J. C.** (1983). Axis determination in eggs of *Xenopus laevis*: A critical period before first cleavage, identified by the common effects of cold, pressure and UV-irradiation. *Dev. Biol.* **99**, 75-87.
- Sato, H., Nagai, T., Kuppaswamy, D., Narishige, T., Koide, M. and Menick, D. R.** (1997). Microtubule stabilization in pressure overload cardiac hypertrophy. *J. Cell Biol.* **139**, 1-11.
- Timasheff and Grisham, L. M.** (1980). In vitro assembly of cytoplasmic microtubules. *Ann. Rev. Biochem.* **49**, 565-591.
- Tsutsui, H., Ishihara, K. and Cooper, G.** (1993). Cytoskeletal role in the contractile dysfunction of hypertrophied myocardium. *Science* **260**, 682-687.
- Tsutsui, H., Tagawa, H., Kent, R. L., McCollam, P. L., Ishihara, K., Nagatsu, M. and Cooper, G.** (1994). Role of microtubules in contractile dysfunction of hypertrophied cardiocytes. *Circulation* **90**, 533-555.
- Vorobjev, I. A., Svitkina, T. M. and Borisy, G. G.** (1997). Cytoplasmic assembly of microtubules in cultured cells. *J. Cell Sci.* **110**, 2635-45.
- Walker, R. A., O'Brien, E. T., Pryer, N. K., Soboeiro, N. F., Voter, W. A., Erickson, H. P. and Salmon, E. D.** (1988). Dynamic instability of individual microtubules: Rate constants and transition frequencies. *J. Cell Biol.* **107**, 1437-1448.
- Wang, X. M., Peloquin, J. J., Zhai, Y., Bulinski, J. C. and Borisy, G. G.** (1996). Removal of MAP4 from MTs in vivo produces no discernible phenotype at the cellular level. *J. Cell Biol.* **132**, 349-358.
- West, R. R., Tenbarger, K. M. and Olmsted, J. B.** (1991). A model for MT-associated protein 4 structure. *J. Biol. Chem.* **266**, 21886-21896.
- Yoshida, T., Imanaka-Toshida, K., Murofushi, H., Tanaka, J., Ito, H. and Inagaki, M.** (1996). Microinjection of intact MAP-4 and fragments induces changes in the cytoskeleton of PtK₂ cells. *Cell Motil. Cytoskel.* **33**, 252-262.
- Yvon, A. M. and Wadsworth, P.** (1997). Non-centrosomal microtubule formation and measurement of minus end microtubule dynamics in A498 cells. *J. Cell Sci.* **110**, 2391-2401.